

# Variation in rms charge radii of deuteron and helium nuclei with $\sqrt{s}$

Sarwat Zahra,  
Bushra Shafaq,  
Bushra Kanwal,  
Nosheen Akbar

**Abstract.** By considering energy-dependent form factors extracted from generalized Chou–Yang model, root mean square (rms) charge radii of deuteron and helium nuclei (alpha) are predicted at different values of center of mass energy which are in good agreement with theoretical predictions and experimental results. The rms radius is inversely proportional to mass of nuclei. Besides, the relationship between radii and energy are also derived.

**Keywords:** Chou–Yang model • Radii

## Introduction

Matter and charge radii of nuclei play a key role in understanding the nuclear physics. Many experimental techniques are used to find the charge and matter radii such as neutron scattering, electron scattering, alpha emission and mirror nuclei isotopic effect. It can also be calculated theoretically using Hartee–Fock–Bogoliubov (HBF) with zero range (Skyrme), HBF with finite range (Gogny), relativistic mean field theory, extended Thomas–Fermi model with Strutinski integral, macroscopic–microscopic approximation and Chou–Yang model. In Chou–Yang model, hadrons are considered to be the cluster of particles that pass through each other during the process of collision [1–4]. Form factors for hadron–hadron scattering, nuclei–nuclei scattering and hadron–nuclei scattering are extracted by using Chou–Yang model [5].

Deuteron and alpha are of great interest for scientists. In the study by Hernandez *et al.* [6] and Sick [7], physicists worked on radii of deuteron and alpha, respectively. Recently, deuteron form factors are calculated in the study by Gross [8] and analysed in the study by Filin *et al.* [9]. In the present study, we calculated the radii of deuteron and alpha at six different values of center of mass (c.m.s.) energy ( $\sqrt{s}$ ) using form factors [5, 10] extracted from Chou–Yang model. The curves for these form factors with respect to energy are also plotted (Figs. 1 and 2).

In 1960s the data regarding low c.m.s. energies of  $\sqrt{s} = 3\text{--}10 \text{ GeV}$  [11] were presented, while in 1970s data at the energies of  $\sqrt{s} = 53\text{--}63 \text{ GeV}$  were reported [12, 13]. In 1980s, the work was done on higher energies in the order of  $10^2 \text{ GeV}$  [14]. By

S. Zahra  
Department of Physics, DS&T  
University of Education  
College Road, Township, Lahore, Punjab, Pakistan

B. Shafaq, B. Kanwal  
CHEP, University of the Punjab  
Quaid e Azam Campus, Lahore, Punjab, Pakistan

N. Akbar<sup>✉</sup>  
Department of Physics, COMSATS  
University Islamabad  
Lahore Campus, Lahore, Punjab, Pakistan  
E-mail: nosheenakbar@culahore.edu.pk

Received: 16 December 2019  
Accepted: 12 May 2020

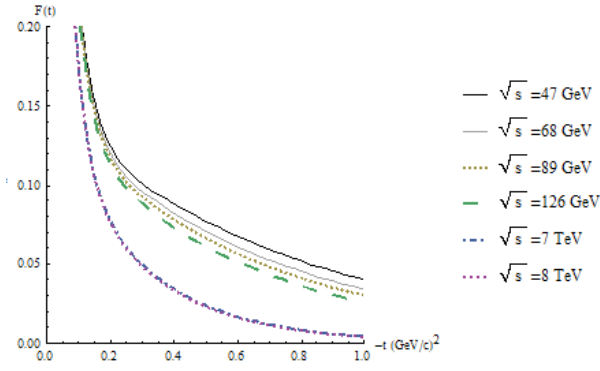


**Fig. 1.** Form factor of deuteron at different values of  $\sqrt{s}$ .

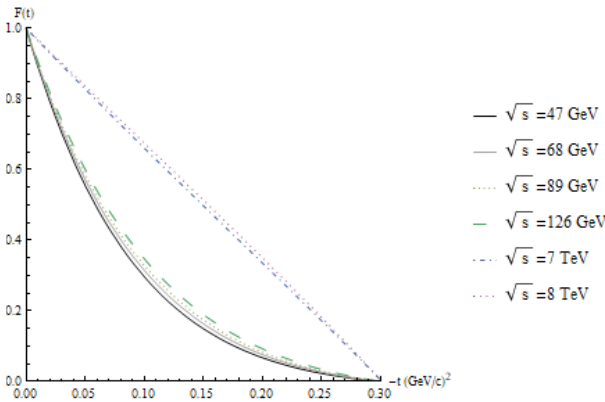


**Fig. 2.** Form factor of helium nucleus at different values of  $\sqrt{s}$ .

the end of the last millennium, the range of available energies ends around 2 TeV. Now results of the TOTEM collaboration at the LHC at  $\sqrt{s} = 7$  TeV and  $\sqrt{s} = 8$  TeV are published [15–17].

In the present article, radii of deuteron and alpha at  $\sqrt{s} = 47, 68, 89, 126$  GeV, 7 and 8 TeV are reported. Using these deuteron and alpha radii, the scattering amplitude and differential cross sections can be calculated. These results for radii are in good agreement with theoretical and experimental results, while in the last section relationship between radii and energy are provided.

### Form factor of deuteron

Several groups worked on elastic electron deuteron scattering [18–21]. Form factor of deuteron was explained as the function of two structure functions  $A(t)$  and  $B(t)$ . These structure functions are considered as the mixture of the electric, magnetic, and quadrupole form factors [22]. The simpler form of the deuteron energy-dependent form factor was proposed in the study by Aleem *et al.* [10] as

$$(1) \quad F(t) = s^{(at+bc^2)} \left( \sum d_i e^{f_i t} e^{ct^2} \right)$$

with  $a = 0.246$ ,  $b = 0.024$ ,  $c = -0.19$ ,  $d_1 = 0.85$ ,  $d_2 = 0.14$ ,  $d_3 = 0.01$ ,  $f_1 = 20.07$ ,  $f_2 = -0.47$ ,  $f_3 = -1.47$  [10].

In Fig. 1, the curves for form factor versus energy ( $\sqrt{s}$ ) are plotted at energies 47, 68, 89 and 126 GeV, 7 and 8 TeV.

### Form factor of alpha

There were many groups that have measured the electromagnetic form factor of alpha at low four momentum transfers [23–26]. The experimental data are parameterized as

$$(2) \quad F_{1\alpha}(t) = \left[ 1 - (a^2 t)^6 \right] e^{-b^2 t}$$

with  $a = 0.316$  fm and  $b = 0.675$  fm [26]. Another relation of the electromagnetic form factor is given as [25]

$$(3) \quad F_{2\alpha}(t) = 0.834 e^{-0.5t} + 0.1655(1 - 0.1157t) e^{-0.1756t}$$

These form factors are used in the geometrical models to calculate the differential cross sections that give satisfactory fit to the experimental data of cross section in the region of low momentum transfer. An energy-dependent form factor of alpha is predicted in the following form [10]:

$$(4) \quad F_\alpha(t) = s^{-0.8t} (1.03e^{14.259t} + 3.25te^{14.738t} - 0.03e^{8.168t})$$

In Fig. 2, the curves for form factor versus energy ( $\sqrt{s}$ ) are plotted at energies 47, 68, 89 and 126 GeV, 7 and 8 TeV.

### Radii of helium and deuteron

With form factors for deuteron and alpha (defined in Eqs. (1) and (4)), rms charge radii are calculated by using the following expression [27]:

$$(5) \quad \langle r^2 \rangle = -6\hbar^2 \frac{dF(t)}{dt} \Big|_{t=0}$$

for energy,  $\sqrt{s} = 47, 68, 89$  and  $126$  GeV, 7 and 8 TeV.

### Results and discussion

In Table 1, the calculated radii are written at different values of energy. It is observed that deuteron radius increases with increase in energy. However, in case of alpha, radius decreases with increase in energy.

These results are in good agreement with the experimental results. It is observed that deuteron nucleus has greater rms radius than alpha meaning that radii depend on the number of nucleons and the strong force among them. If there is more number of nucleons, there will be stronger binding inside the nucleus, decreasing the size of the nucleus. In Fig. 3, a curve is plotted between rms radii of deuteron and  $\sqrt{s}$ .

The relationship between the rms radii and the energy is found by fitting the radii at 47, 68, 89 and 126 GeV with the following expression:

$$(6) \quad \sqrt{\langle r^2 \rangle} = \omega_1 \ln(\sqrt{s}) + \omega_2$$

We found  $\omega_1 = 0.06262 \pm 0.000078$  fm and  $\omega_2 = 1.9951 \pm 0.000148$  fm. The rms radii calculated by Eq. (6) at 7 and 8 TeV give the same results as given

**Table 1.** The rms radii of deuteron and alpha

Element	$\sqrt{s}$ [GeV]	Experimental rms radii	Radii (fm) [7]	Radii (fm) [28]	Our calculated rms radii (fm)	Authors' thesis (fm) [29]
Deuteron	47				2.09984	2.09984
	68				2.10992	2.10992
	89	$1.9566 \pm 0.0019$	$2.130 \pm 0.010$	2.12562 (78)	2.11724	2.11724
	126	[30]			2.12666	2.12666
	7000				2.23259	–
Alpha	8000				2.23602	–
	47		$1.681 \pm 0.0004$		1.63990	1.63990
	68		–		1.59725	1.59725
	89	1.57 [31]	–		1.56544	1.56544
	126		–		1.52337	1.52337
7000			–		0.904946	–
	8000		–		0.876933	–

in Table 1. So with Eq. (6), we can predict radii at any value of energy.

In Fig. 4, alpha radii are plotted against the c.m.s. energy,  $\sqrt{s}$ .

The relation between the rms radii of alpha and the energy is found by fitting the radii at 47, 68, 89 and 126 GeV, 7 and 8 TeV with the following expression:

$$(7) \quad \sqrt{\langle r^2 \rangle} = \omega_{11} \ln(\sqrt{s}) + \omega_{22}$$

We found  $\omega_{11} = -0.346445 \pm 0.00523$  fm and  $\omega_{22} = 2.234889 \pm 0.0014242$  fm. The rms radii calculated with Eq. (7) at 7 and 8 TeV give the same results as given in Table 1. So with Eq. (7), we can predict radii at any value of energy.

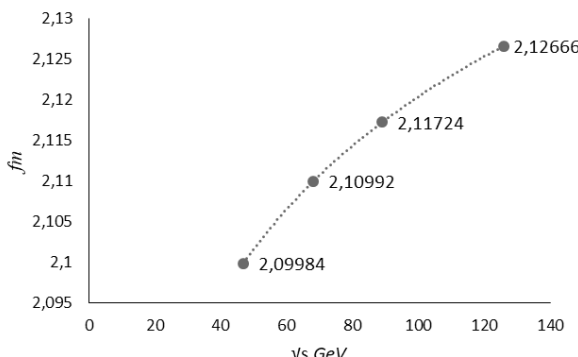


**Fig. 3.** Graph between rms radii of deuteron at different centers of mass energy.

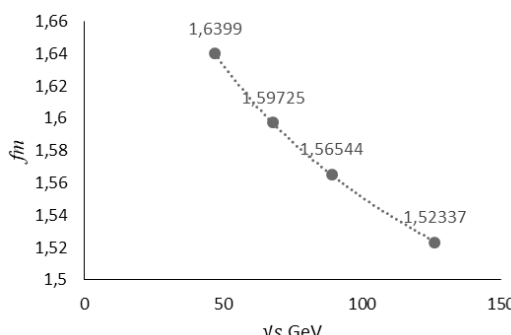


**Fig. 4.** Graph between rms radius of alpha nucleus and the center of mass energy.

## Conclusions

The results in Table 1 clearly indicate that the radius of deuteron and alpha nuclei are energy-dependent. It can also be inferred that mass is inversely proportional to rms radii. It is also concluded that radii decrease with the increase in number of nucleons.

## References

- Chou, T. T., & Yang, C. N. (1968). Model of elastic high-energy scattering. *Phys. Rev.*, *170*, 1591–1596. DOI: 10.1103/PhysRev.170.1591.
- Chou, T. T., & Yang, C. N. (1968). Possible existence of kinks in high-energy elastic pp scattering cross section. *Phys. Rev. Lett.*, *20*, 1213–1215. <https://journals.aps.org/prl/abstract/10.1103/PhysRevLett.20.1213>.
- Lo, S. Y., & Yang-Guo, L. (1983). Transverse-momentum spectrum of inclusive reactions in the geometrical picture. *Phys. Rev. D*, *28*, 2756–2761. <https://doi.org/10.1103/PhysRevD.28.2756>.
- Glauber, R. J., & Velasco, J. (1984). Multiple diffraction theory of pp scattering at 546 GeV. *Phys. Lett. B*, *147*, 380–384. [https://doi.org/10.1016/0370-2693\(84\)90137-0](https://doi.org/10.1016/0370-2693(84)90137-0).
- Saleem, M., Fazal-e-Aleem, , & Azhar, I. A. (1988). Generalized Chou-Yang model for p(p)-p and  $\Lambda(\Lambda)$ -p elastic scattering at high energies. *Europhys. Lett.*, *6*(3), 201–206. <https://doi.org/10.1209/0295-5075/6/3/003>.
- Hernandez, O. J., Ekström, A., Dinur, N., Ji, C., Bacca, S., & Barnea, N. (2018). The deuteron-radius puzzle is alive: A new analysis of nuclear structure uncertainties. *Phys. Lett. B*, *778*, 377–383. DOI: 10.1016/j.physletb.2018.01.043.
- Sick, I. (2015). Form factors and radii of light nuclei. *J. Phys. Chem. Ref. Data*, *44*, 031213. DOI: 10.1063/1.4921830.
- Gross, F. (2020). Covariant spectator theory of np scattering: Deuteron form factors. *Phys. Rev. C*, *101*(2), 024001. <https://doi.org/10.1103/PhysRevC.101.024001>.
- Filin, A. A., Baru, V., Epelbaum, E., Krebs, H., Möller, D., & Reinert, P. (2020). Extraction of the neutron charge radius from a precision calculation of the deuter-

- on structure radius. *Phys. Rev. Lett.*, **124**(8), 082501. <https://doi.org/10.1103/PhysRevLett.124.082501>.
10. Aleem, F., Ali, S., & Saleem, M. (1995). Nucleas (hadron) nucleus elastic scattering and geometrical picture. *Hadronic Journal*, **18**(4), 353–372. Available from [https://inis.iaea.org/search/search.aspx?orig\\_q=RN:28020207](https://inis.iaea.org/search/search.aspx?orig_q=RN:28020207).
  11. Besliu, C., Besliu, T., Constantinescu, A., Gavrilas, M., Mihul, A., Gheordanescu, N., Hangea, N., Teleman, M., Teodorescu, L., Tipa, I., Karnauhov, V., Moroz, V., & Nefedeva, L. (1969). Neutron-proton elastic scattering from 3 to 10 GeV. *Nuovo Cimento Soc. Ital. Fis. A-Nucl. Part. Fields*, **59**, 1–8. <https://doi.org/10.1007/BF02756339>.
  12. Goggi, G., Livan, M., Cavalli-Sforza, M., Mantovani, G. C., Fraternali, M., Pastore, F., Conta, C., Rossini, B., & Alberi, G. (1978). Evidence for inelastic propagators in proton-deuteron elastic scattering at  $\sqrt{s} = 63$  GeV. *Phys. Lett. B*, **77**, 428–432. DOI: 10.17182/hepdata.27425.
  13. Goggi, G., Sforza, M. C., Conta, C., Fraternali, M., Livan, M., Mantovani, G. C., Pastore, F., Rossini, B., & Alberi, G. (1978). Observation of a narrow minimum and of inelastic shadow effects in deuteron-deuteron elastic scattering at  $\sqrt{s} = 53$  GeV. *Phys. Lett. B*, **77**, 433–437. DOI: 10.17182/hepdata.27432.
  14. Ambrosio, M., Anzivino, G., Barbarino, G., Becker, U., Carboni, G., Cavasinni, V., Del Prete, T., Kantardjian, G., Owen, D. L., Morganti, M., & Paradiso, J. (1982). Measurements of elastic scattering in alpha-alpha and alpha-proton collisions at the CERN intersecting storage rings. *Phys. Lett. B*, **113**, 347–352. [https://doi.org/10.1016/0370-2693\(82\)90054-5](https://doi.org/10.1016/0370-2693(82)90054-5).
  15. Antchev, G., Aspell, P., Atanassov, I., Avati, V., Baechler, J., Berardi, V., Berretti, M., Bozzo, M., Brücken, E., Buzzo, A., Cafagna, F. S., Calicchio, M., Catanesi, M. G., Covault, C., Csanád, M., Csörgő, T., Deile, M., Dimovasili, E., Doubek, M., Eggert, K., Eremin, V., Ferro, F., Fiergolski, A., Garcia, F., Giani, S., Greco, V., Grzanka, L., Heino, J., Hilden, T., Janda, M., Kašpar, J., Kopal, J., Kundrat, V., Kurvinen, K., Lami, S., Latino, G., Lauhakangas, R., Leszko, T., Lippmaa, E., Lokajíček, M., Lo Vetere, M., Lucas Rodríguez, F., Macrì, M., Magaletti, L., Magazzù, G., Mercadante, A., Minutoli, S., Nemes, F., Niewiadomski, H., Noschis, E., Novák, T., Oliveri, E., Oljemark, F., Orava, R., Oriunno, M., Österberg, K., Perrot, A. -L., Palazzi, P., Pedreschi, E., Petäjäjärvi, J., Procházka, J., Quinto, M., Radermacher, E., Radicioni, E., Ravotti, F., Robutti, E., Ropelewski, L., Ruggiero, G., Saarikko, H., Santroni, A., Scribano, A., Sette, G., Snoeys, W., Spinella, F., Sziklai, J., Taylor, C., Turini, N., Vacek, V., Vitek, M., Welti, J., Whitmore, J., & TOTEM Collaboration. (2011). Proton-proton elastic scattering at the LHC energy of  $\sqrt{s}=7$ TeV. *Europhys. Lett.*, **95**, 41001. <https://doi.org/10.1209/0295-5075/95/41001>.
  16. Antchev, G., Aspell, P., Atanassov, I., Avati, V., Baechler, J., Berardi, V., Berretti, M., Bossini, E., Bozzo, M., Brogi, P., Brücken, E., Buzzo, A., Cafagna, F. S., Calicchio, M., Catanesi, M. G., Covault, C., Csanád, M., Csörgő, T., Deile, M., Eggert, K., Eremin, V., Ferretti, R., Ferro, F., Fiergolski, A., Garcia, F., Giani, S., Greco, V., Grzanka, L., Heino, J., Hilden, T., Intonti, R. A., Kašpar, J., Kopal, J., Kundrat, V., Kurvinen, K., Lami, S., Latino, G., Lauhakangas, R., Leszko, T., Lippmaa, E., Lokajíček, M., Lo Vetere, M., Lucas Rodríguez, F., Macrì, M., Mercadante, A., Minutoli, S., Naaranjoa, T., Nemes, F., Niewiadomski, H., Oliveri, E., Oljemark, F., Orava, R., Oriunno, M., Österberg, K., Palazzi, P., Palocko, L., Passaro, V., Peroutka, Z., Petrizzelli, V., Politi, T., Procházka, J., Prudenzao, F., Quinto, M., Radermacher, E., Radicioni, E., Ravotti, F., Robutti, E., Ropelewski, L., Ruggiero, G., Saarikko, H., Scribano, A., Smajek, J., Snoeys, W., Sodzawiczny, T., Sziklai, J., Taylor, C., Turini, N., Vacek, V., Welti, J., Wyszkowski, P., Zielinski, K., & TOTEM Collaboration. (2015). Evidence for non-exponential elastic proton-proton differential cross-section at low  $|t|$  and  $s=8$ TeV by TOTEM. *Nucl. Phys. B*, **899**, 527–546. DOI: 10.1016/j.nuclphysb.2015.08.010.
  18. Buchanan, C. D., & Yearian, M. R. (1965). Elastic electron-deuteron scattering and possible meson-exchange effects. *Phys. Rev. Lett.*, **15**, 303–306. <https://doi.org/10.1103/PhysRevLett.15.303>.
  19. Elias, J. E., Friedman, J. I., Hartmann, G. C., Kendall, H. W., Kirk, P. N., Sogard, M. R., Van Speybroeck, L. P. & De Pagter, J. K. (1969). Measurements of elastic electron-deuteron scattering at high momentum transfers. *Phys. Rev.*, **177**, 2075–2092. DOI: 10.1103/PhysRev.177.2075.
  20. Galster, S., Klein, H., Bleckwenn, J., Wegener, D., Moritz, J., & Schmidt, K. H. (1971). Elastic electron-deuteron scattering and the electric neutron form factor at four-momentum transfers  $5 \text{ fm}^{-2} < q^2 < 14 \text{ fm}^{-2}$ . *Nucl. Phys.*, **32**, 221–237. DOI: 10.1016/0550-3213(71)90068-X.
  21. Arnold, R. G., Chertok, B. T., Dally, E. B., Grigorian, A., Jordan, C. L., Schütz, W. P., Zdarko, R., Martin, F., & Mecking, B. A. (1975). Measurement of the electron-deuteron elastic-scattering cross section in the range  $0.8 < \sim q^2 < \sim 6 \text{ GeV}^2$ . *Phys. Rev. Lett.*, **35**, 776–779. <https://doi.org/10.1103/PhysRevLett.35.776>.

22. Friedman, J. I., Kendall, H. W., & Gram, P. A. M. (1960). Experimental study of the magnetic structure of the neutron. *Phys. Rev.*, *120*, 992–999. <https://doi.org/10.1103/PhysRev.120.992>.
23. Erich, U., Frank, H. E., Haas, D., & Prange, H. (1971). Elastic electron scattering on  ${}^4\text{He}$  at energies between 30 and 59 MeV. *Z. Phys.*, *209*, 208–218. DOI: [10.1007/BF01395278](https://doi.org/10.1007/BF01395278).
24. Frosch, R. F., McCarthy, J. S., Rand, R. E., & Yearian, M. R. (1967). Structure of the  ${}^4\text{He}$  nucleus from elastic electron scattering. *Phys. Rev.*, *160*, 874–879. <https://doi.org/10.1103/PhysRev.160.874>.
25. McCarthy, J. S., Sick, I., & Whitney, R. R. (1977). Electromagnetic structure of the helium isotopes. *Phys. Rev. C*, *15*, 1396–1414. <https://doi.org/10.1103/PhysRevC.15.1396>.
26. Lombard, R. J., & Tellez-Arenas, A. (1985). Proton- ${}^4\text{He}$  elastic scattering in the Chou-Yang model. *Phys. Lett. B*, *165*, 205–208. [https://doi.org/10.1016/0370-2693\(85\)90721-X](https://doi.org/10.1016/0370-2693(85)90721-X).
27. Menon, M. J. (1993). Elementary amplitudes in the multiple diffraction theory of pp and ppbar elastic scattering. *Phys. Rev. D*, *48*, 2007–2018. <https://doi.org/10.1103/PhysRevD.48.2007>.
28. Pohl, R., Nez, F., Fernandes, L. M., Amaro, F. D., Biraben, F., Cardoso, J. M., Covita, D. S., Dax, A., Dhawan, S., Diepold, M., & Giesen, A. (2016). Laser spectroscopy of muonic deuterium. *Science*, *353*, 669–673. DOI: [10.1126/science.aaf2468](https://doi.org/10.1126/science.aaf2468).
29. Zahra, S. (2011). *Geometrical pictures, QCD and radii of hadrons/lighter nuclei*. Unpublished PhD Thesis, University of the Punjab.
30. Buchmann, A. J., Henning, H., & Sauer, P. U. (1996). Meson and quark degrees of freedom and the radius of the deuteron. *Few-Body Syst.*, *21*, 149–165. <https://doi.org/10.1007/s006010050045>.
31. Ogawa, Y., Toki, H., Tamenaga, S., Sugimoto, S., & Ikeda, K. (2006). Charge and parity projected relativistic mean field model with pion for finite nuclei. *Phys. Rev. C*, *73*, 034301–034312. <https://doi.org/10.1103/PhysRevC.73.034301>.